Simulation and Optimization of Coal Gasification in a Moving-bed Reactor to Produce Synthesis Gas Suitable for Methanol Production Unit

M. Shamsi,[a] H. Ale Ebrahim,[a] and M. J. Azarhoosh[b,*]
[a]Department of Chemical Engineering, Amirkabir University of Technology (Tehran Polytechnic), Tehran, Iran
[b]Department of Chemical Engineering, Faculty of Engineering, Urmia University, Urmia, Iran

https://doi.org/10.15255/CABEQ.2019.1673

Original scientific paper
Received: May 23, 2019
Accepted: November 29, 2019

This paper presents process simulation and optimization of coal gasification process in a moving-bed reactor using Pittsburgh No. 8 coal as feed. The system of differential equations for the mass and energy balances was solved using 4th-order Runge-Kutta method and optimized by non-dominated sorting genetic algorithm-II (NSGA-II) method. The simulation was used to predict solid and gas temperature profile and gas composition along the reactor. The simulation results were compared successfully with experimental data relevant to Westfield plant in Scotland. In addition, the effect of operating parameters such as coal-to-oxygen molar ratio, steam-to-oxygen molar ratio, inlet gas temperature, reactor pressure, and oxygen mole fraction in inlet air on amount of synthesis gas (syngas) production, hydrogen to carbon monoxide molar ratio (HCMR) in produced syngas, and coal conversion was investigated. Finally, the reactor performance was optimized to produce the highest syngas production with a HCMR of two using NSGA-II method.

Keywords:
moving-bed reactor, coal gasification, simulation, optimization, methanol, synthesis gas

Introduction

Gasification is considered one of the most efficient technologies for the conversion of low-cost coal into clean and highly priced chemicals, fuels, and power[1,2]. The major product of the coal gasification process to coal gas is hydrogen and carbon monoxide, known as synthesis gas (syngas)[3,4]. In recent years, the considerable increase in the price of crude oil and natural gas has focused attention on whether fuel for power production and feedstock for the chemical industry could be obtained from the gasification of coal[5,6]. The syngas produced by coal gasification contains H_2 and CO to produce methanol. Methanol can be used directly as automotive fuel or converted to gasoline or light olefins[7–10]. Gasification is performed in different types of reactors, depending on the type of solid-gas contact: moving-bed reactor, fluidized-bed reactor or entrained-flow reactor. The higher residence time and countercurrent flow in moving-bed reactor favor higher carbon conversion as compared to fluidized-bed and entrained-flow reactors[1,11]. In these reactors, the coal is fed through the top of the reactor and flows downward under gravity. Moving-bed reactor is usually operated below the ash fusion temperature (AFT) to avoid clinkering of the coal. The gasifying agents are fed in from the bottom and come into contact with the solid as they move upward[12]. As the coal flows downward, it undergoes a series of different reactions that include drying, devolatilization, gasification, and combustion (Fig. 1)[13]. The gasification and combustion of char involves a series of heterogeneous reactions with oxygen and steam.

The following reactions occur during this stage[1]:

Combustion:

$$\lambda\, C + O_2 \rightarrow 2(\lambda - 1)\, CO + (2 - \lambda)\, CO_2 \qquad (1)$$

Char gasification reaction:

$$C + H_2O \rightarrow CO + H_2 \qquad (2)$$

Boudouard reaction:

$$C + CO_2 \rightarrow 2CO \qquad (3)$$

Methanation reaction:

$$C + 2H_2 \rightarrow CH_4 \qquad (4)$$

---

[*]Corresponding author: Mohammad Javad Azarhoosh
E-mail: mj.azarhoosh@urmia.ac.ir, Tel: +98 44 3194 2893

Water-gas shift reaction:

$$CO + H_2O \rightarrow CO_2 + H_2 \qquad (5)$$

where λ in reaction (1) is equal to 1 for particles larger than 1 mm. For fast reactions, diffusion is the rate-controlling step, while the rate-controlling step for slow reactions is the surface reactions within the pores of particles[14].

Yoon *et al.*[15] modeled a moving-bed reactor with a coal gasification process in a steady state, at which gas temperature was considered equal to solid temperature, and Illinois coal was considered as feed. They found that the maximum temperature inside the reactor was significant, and was determined by the ratio of steam to oxygen at the entrance to the reactor. Wen *et al.*[14] developed a complex computer model to simulate their experimental work performed earlier on the gasification of coal in a moving-bed reactor, and they assumed the solid and gas temperatures to be equal. Composition of outlet gas from the gasifier was compared with the experimental data. Kulkarni and Ganguli[1] simulated the same system with system of Wen *et al.*, to study the effect of variables such as reactor pressure and steam-to-carbon ratio using subbituminous coal in the Aspen program, and concluded that with increasing reactor pressure, the gas composition of the product remained constant, but with increasing steam-to-carbon ratio the carbon monoxide mole fraction had reduced and carbon dioxide mole fraction had increased. Singh *et al.*[16] developed a mathematical model of coal gasification process in Lurgi gasifier. The validated model was used to study the effect of operating parameters such as mole fraction of oxygen in air stream, steam flow rates, and pressure of the gasification system. Results indicate that the value of oxygen mole fraction around 0.42 in air stream can provide optimum performance in oxygen-based gasification systems. Longitudinal profiles of solid and gas temperatures, and particularly the peak temperature in the reactor, are basic parameters for operating a Lurgi gasifier, since the solid peak temperature in the reactor must not at any time go as high as the ash softening point[12]. The AFT for Pittsburgh No.8 is 1366 K, therefore it is necessary to simulate Lurgi gasifier with discrete temperature profiles to obtain exact maximum temperature of solid phase and check the possibility of reducing steam consumption while maintaining the ash state in order to optimize the reactor's performance. After simulating the reactor, the reactor performance was optimized to produce the highest syngas yield with a defined hydrogen to carbon monoxide ratio (HCMR) of 2 or maximum syngas yield.

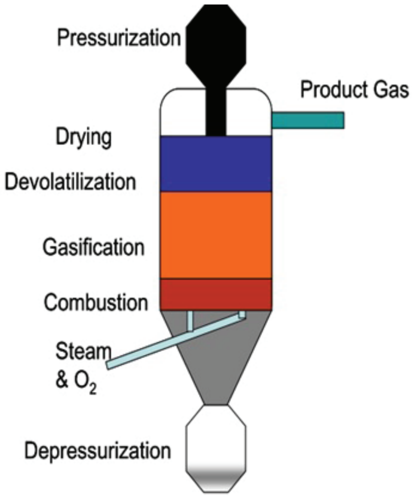

Fig. 1 – *Sections of coal gasification moving-bed reactor*[13]

The main objective of the present study was process simulation and optimization of coal gasification process in a moving-bed reactor to produce synthesis gas suitable for methanol production unit. The differential mass and energy balance equations were solved using 4th-order Runge-Kutta method, and optimized by non-dominated sorting genetic algorithm-II (NSGA-II) method. Firstly, the simulation results were compared with experimental data relevant to Westfield plant in Scotland. Next, the effect of operating parameters such as coal-to-oxygen molar ratio, steam-to-oxygen molar ratio, inlet gas temperature, reactor pressure, and oxygen mole fraction in inlet air on mole fraction and HCMR of produced syngas and coal conversion was investigated. Finally, the reactor performance was optimized to produce the highest syngas production with a HCMR of 2 using NSGA-II method. Although there are published articles in the field of simulation of coal gasification in moving-bed reactors, the main novelties of the present study are:

– Investigation of the effect of operating parameters on the reactor performance

– Consideration of separate temperatures for gas and solid phases to determine the maximum solid phase temperature

– Application of the kinetics of all possible reactions

– Simultaneous use of shrinking core and volume models in the different reactor areas

– Calculation of the distribution of gas components in the pyrolysis zone

– Optimization of coal gasification in moving-bed reactor to produce synthesis gas suitable for methanol production unit.

Model description

In this study, a simulation of a stationary state system with temperature distribution for both the solid and gas phase is performed. Shrinking unreacted core model and volume reaction model were used to describe the solid-gas reactions. Assumptions in the model were as follows.

a) Steady state is assumed.

b) Plug flow is assumed both for coal and gas.

c) Residence time of coal in drying and pyrolysis section is assumed to be negligible as compared to combustion-gasification section.

d) The pressure drop in the gasifier is neglected.

e) Bulk reaction is assumed for all gas-solid reactions except char combustion, which is treated according to shrinking unreacted core model.

Due to the porosity of coal particles and the slowness of the gasification reactions, these reactions were carried out in the bulk of the solid particless. However, due to the rapid combustion reaction, this reaction was performed on the surface of the solid particles only, thus the oxygen molecules could not penetrate the particles; so solid particles from top to bottom come up with two types of reaction model (bulk reaction model in gasification zone and shrinking unreacted core model in the combustion zone); this is one of the differences with other models. The model was used to predict the composition of product gas, temperature profiles for both solid and gas phases, and effect of process variables on the syngas composition.

Reaction kinetics

The kinetics of reactions occurring inside the reactor is listed in Table 1[14–19].

Mass and energy balance

The differential equations derived from the mass balance based on molar flux are as follows:

$$\frac{\mathrm{d}F_{\mathrm{H_2}}}{\mathrm{d}z} = -R_2 + 2R_4 + R_5 \tag{6}$$

$$\frac{\mathrm{d}F_{\mathrm{CO}}}{\mathrm{d}z} = \frac{2(\lambda - 1)}{\lambda} R_1 + R_2 + 2R_3 - R_5 \tag{7}$$

$$\frac{\mathrm{d}F_{\mathrm{H_2O}}}{\mathrm{d}z} = -R_2 - R_5 \tag{8}$$

$$\frac{\mathrm{d}F_{\mathrm{CO_2}}}{\mathrm{d}z} = \frac{2-\lambda}{\lambda} R_1 - R_3 + R_5 \tag{9}$$

$$\frac{\mathrm{d}F_{\mathrm{O_2}}}{\mathrm{d}z} = -\frac{1}{\lambda} R_1 \tag{10}$$

$$\frac{\mathrm{d}F_{\mathrm{N_2}}}{\mathrm{d}z} = 0 \tag{11}$$

$$\frac{\mathrm{d}F_{\mathrm{CH_4}}}{\mathrm{d}z} = R_4 \tag{12}$$

$$\frac{\mathrm{d}F_{\mathrm{C}}}{\mathrm{d}z} = -R_1 - R_2 - R_3 - R_4 \tag{13}$$

where F is molar flux, and z is height of reactor. The following equations are obtained from balance of energy considering radiation and convection as mechanisms of heat transfer[12,20,21].

Table 1 – *Kinetics of reactions occurring inside the reactor*

Reaction	Kinetic
Carbon-oxygen reaction	$R_1 = \dfrac{P_{\mathrm{O_2}}}{\dfrac{1}{k_{film}} + \dfrac{1}{k_{ash}}}$
Carbon-steam reaction	$R_2 = k_2\left(P_{\mathrm{H_2O}} - P_{\mathrm{H_2O}}{}^{*}\right)[\mathrm{C}]$
Boudouard reaction	$R_3 = k_3\left(P_{\mathrm{CO_2}} - P_{\mathrm{CO_2}}{}^{*}\right)[\mathrm{C}]$
Methanation reaction	$R_4 = k_4\left(P_{\mathrm{H_2}} - P_{\mathrm{H_2}}{}^{*}\right)[\mathrm{C}]\mathrm{e}^{\left(-7.087 - \frac{8078}{T}\right)}$
Water-gas shift reaction	$R_5 = 2.87 \cdot 10^5 b \mathrm{e}^{\frac{-27760}{RT}} \left(X_{\mathrm{CO}} - \dfrac{X_{\mathrm{CO_2}} X_{\mathrm{H_2}}}{X_{\mathrm{H_2O}} K_{WGS}}\right) X_{ash} \rho_{\mathrm{C}} \left(1 - \varepsilon_{bed}\right) P^{\left(0.5 - \frac{P}{250}\right)} \mathrm{e}^{\left(-8.91 + \frac{5553}{T}\right)}$

$$\left(C_{Ps}F_s+\frac{4\sigma}{\frac{2}{e}-1}T_s^3\right)\frac{\mathrm{d}T_s}{\mathrm{d}z}=-h_P n_P A_P\left(T_s-T_g\right)-\sum_{i=1}^{4}\Delta H_i R_i T_s-\sum_{i=1}^{4}\sum_{j=1}^{N}a_{ij}R_i\left[H_j\left(T_s\right)-H_j\left(T_g\right)\right] \qquad (14)$$

where e equal to 0.9 is emissivity of coal, σ is Stefan-Boltzmann constant, a_{ij} is stoichiometric coefficient of gas reactant j in reaction of i, h_p is gas-solid heat transfer coefficient, n_p is number of solid particles in unit of volume, A_p is surface area of a particle, and H is enthalpy[12,20,21].

$$\frac{\mathrm{d}T_g}{\mathrm{d}z}=\frac{1}{C_{Pg}F_g}\left[h_P n_P A_P\left(T_s-T_g\right)-\Delta H_5 R_5\left(T_g\right)+\sum_{i=1}^{4}\sum_{j=1}^{N}b_{ij}R_i\left[H_j\left(T_s\right)-H_j\left(T_g\right)\right]-hS\left(T_g-T_W\right)\right] \qquad (15)$$

where b_{ij} is stoichiometric coefficient of products in gas phase. The above mathematical model of the coal gasification moving-bed reactor leads to a set of nonlinear ordinary differential equations with a set of split boundary conditions. These differential equations were solved using a Runge–Kutta method called shooting method. Shooting method transforms the boundary value problem into an initial value problem, and then the resulting equations are solved by the Runge–Kutta method.

Optimization method (genetic algorithm)

The classical methods, such as Goal-Programming Method and Goal-Attainment Method or evolutionary methods including genetic algorithm (GA), particle swarm optimization (PSO), and ant colony (ACO) algorithm can be used in optimization[22]. In recent years, evolutionary algorithms have been much more effective in solving complex problems compared to the classic methods, with the GA being one of the most important and most widely used fields of evolutionary methods[23]. GA is one of the random search algorithms, the idea of which has been derived from nature and Darwin's theory. These algorithms are widely employed in solving optimization problems. In nature, more suitable generations are formed from more suitable chromosomes. Meanwhile, some mutations occur in the chromosomes, which may result in better future generations. GA is used to solve problems using this idea[24]. Table 2 indicates the characteristics applied in the GA code of this study.

Results and discussion

Model validation

The model utilized operating parameters of Wesfield plant in Scotland for Pittsburgh No. 8 coal as feed (Table 3)[14]. The simulation results compared with the experimental results on Pittsburgh coal are presented in Table 4[14].

Table 2 – *Properties of GA used in this study*

Parameter	Value	Parameter	Value
Number of generations	20,000	Crossover method	Arithmetic method
Population size	100	Crossover probability	0.75
Parent selection method	Tournament selection	Mutation method	Gaussian method
Tour size	15	Mutation probability	0.25

Table 3 – *Lurgi gasifier operating conditions of Westfield unit in Scotland for Pittsburgh No. 8 coal*

Parameter	Value	Parameter	Value
Flow rate of coal (kg s^{-1})	1.02	Temperature of inlet gas (K)	644
Flow rate of steam (kg s^{-1})	3.29	Temperature of inlet solid (K)	298
Flow rate of oxygen (kg s^{-1})	0.63	Temperature of reactor wall (K)	644
Oxygen mole fraction in air	0.94	Bed voidage	0.4
Bed pressure (kPa)	2500	Bed diameter (m)	3.05
size of solid particle (m)	0.02	Bed height (m)	3.05

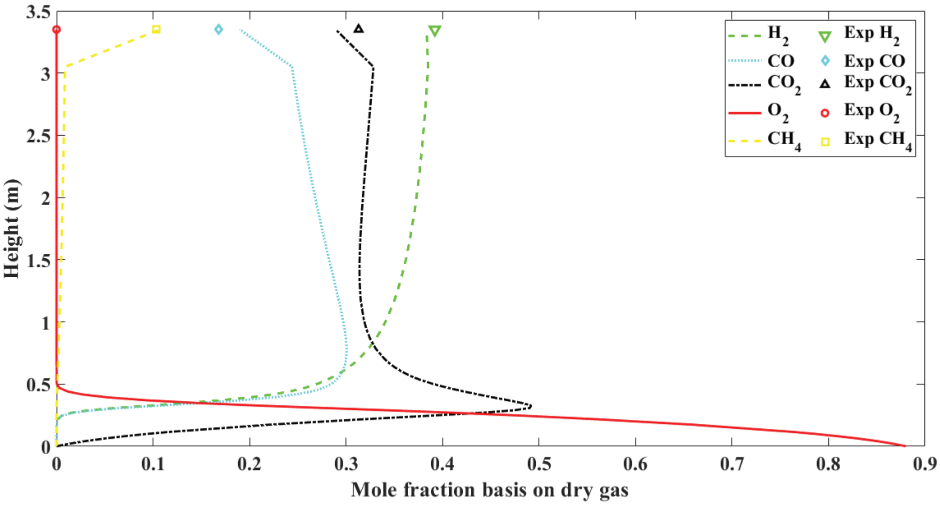

Fig. 2 – *Mole fraction of gas components along the reactor on dry gas basis*

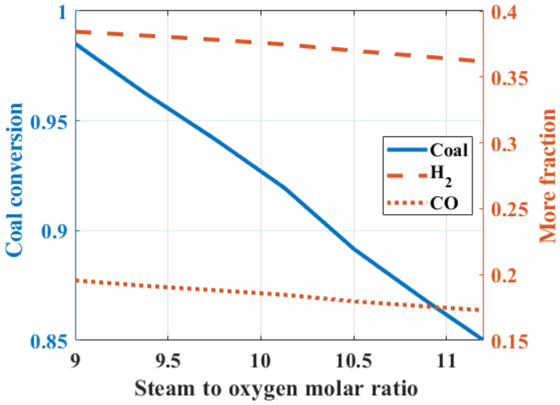

Fig. 3 – *Effects of SOR on outlet solid conversion and synthesis gas composition*

Table 4 – *Comparison between simulation and plant data for Pittsburgh No. 8 coal*

Parameter	Plant data	Simulation results	Relative error (%)
Flow rate of dry product gas (mol s^{-1})	97.1	95.2	1.95
Carbon conversion	0.989	0.987	0.20
Flow rate of oulet steam (mol s^{-1})	149	155	4.02
H_2 (% mol basis on dry gas)	39.20	38.75	1.14
CO (% mol basis on dry gas)	16.80	17.23	2.55
CO_2 (% mol basis on dry gas)	31.30	31.25	0.16
CH_4 (% mol basis on dry gas)	10.30	10.40	0.97
N_2 (% mol basis on dry gas)	1.60	1.65	3.12
H_2S (% mol basis on dry gas)	0.70	0.72	2.85

Fig. 2 shows the mole fraction of gas components on dry gas basis as a function of reactor length. In other reports, a diagram on wet gas basis has been shown throughout the reactor, which could hardly distinguish the areas of combustion and conversion of coal to gas. However, in this figure, the combination of dry gas basis diagram with the maximum point for carbon dioxide content can be convenient to distinguish the different sections of the reactor. However, the most fundamental difference between this figure and gas concentration diagrams in previous studies is in displaying the pyrolysis stage at the top of the reactor. This figure also compares the composition of the simulated output gas with the experimental output gas composition (hollow circles) to validate the results of the simulation. The results indicate a good agreement between simulation results and experimental data.

Effects of operating parameters

Effect of steam-to-oxygen molar ratio (SOR)

Fig. 3 shows the effect of SOR on the conversion of carbon at bottom of reactor and the mole fraction of syngas at top of the reactor, respectively. As it may be observed from Fig. 3, an increase in the carbon conversion and syngas production may be achieved by reducing SOR. In other words, the rate of endothermic gasification reactions, and as a result, carbon conversion, is reduced by increasing SOR (decreasing oxygen ratio).

Effect of coal-to-oxygen molar ratio (COR)

Fig. 4 shows the effect of increasing COR on the carbon conversion and produced syngas composition. As shown in Fig. 4, the increase in COR value, which is also representative of the reactor capacity, reduced the conversion efficiency (similar to SOR effect), but had no effect on the syngas composition of the product (because steam and oxygen values had not changed). In the other words, the increase in reactor capacity had no significant effect on the composition of the produced syngas.

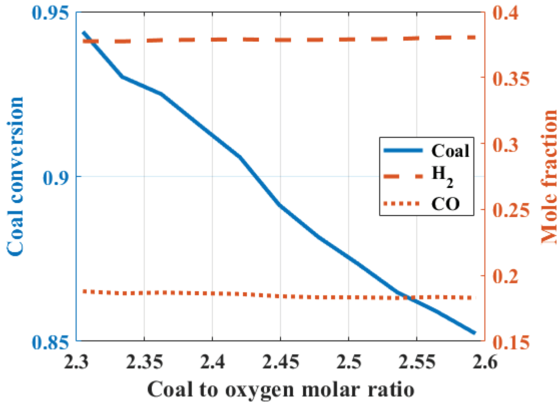

Fig. 4 – *Effects of COR on outlet solid conversion and synthesis gas*

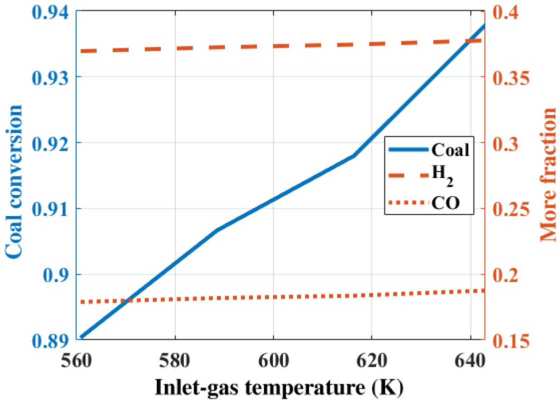

Fig. 5 – *Effects of inlet-gas temperature on outlet solid conversion and syngas composition (reactor pressure = 23.8 atm)*

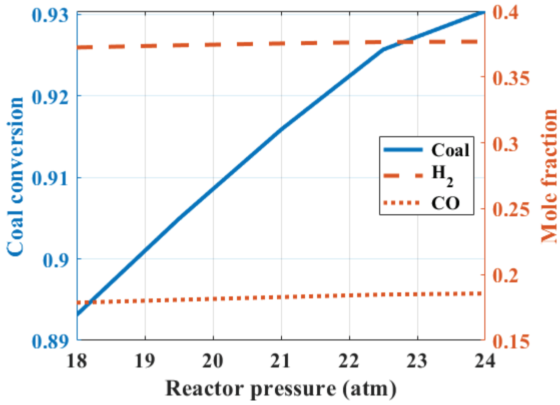

Fig. 6 – *Effects of reactor pressure on outlet solid conversion and syngas composition (inlet gas temperature = 644 K)*

Effect of inlet gas temperature

At a temperature below the critical gas temperature, the reactor does not function properly and carbon exits as waste in its raw form, and is not converted completely into gas[19]. The increase in the temperature of the inlet gas has a favorable effect on the reactor's performance, which increases the conversion of solids and amount of syngas because the reactions of coal gasification zone are endothermic. Therefore, inlet gas temperature is an important operating variable for estimating the process efficiency and reactor performance. Therefore, it is possible to compensate for the reduction of gas by increasing the temperature, but it is costly and irrational in comparison to SOR reduction. Fig. 5 shows the effect of increasing the temperature of the inlet gas temperature on the syngas composition, as evidenced by the increase in the temperature of the inlet gas, which increases the syngas content, including the content of hydrogen and carbon monoxide.

Effect of reactor pressure

The reactor pressure is usually chosen based on the type o reactor and the final use of the gas product. Fig. 6 shows the effect of reactor pressure on the outlet conversion of solids and syngas composition. By increasing pressure from 18 to 25 atm, the hydrogen and carbon monoxide content in the produced syngas is also increased.

Effect of oxygen mole fraction in inlet-air

In the production of medium-Btu gas (such as that used for methanol production), pure oxygen is used rather than air as combustion agent, and by decreasing oxygen mole fraction in oxidizer stream, the produced gas goes to a hydrogen-rich composition. The oxygen mole fraction less than 0.6 results in HCMR that is significantly higher than the optimal value of 2, and therefore not suitable for methanol production[25]. Fig. 7 shows the effect of oxygen mole fraction in air stream on outlet carbon conversion and components mole fraction in syngas. By increasing the oxygen mole fraction, the rate of exothermic combustion reactions also increased, thus increasing the reactor temperature and providing the heat of endothermic coal gasification reactions.

Optimization

If the product gas is to be used to produce methanol, the molar ratio of HCMR in the dry gas should be set to 2. Therefore, by optimizing the reactor's performance, it is possible to achieve this goal. A NSGA-II was used to optimize and obtain Pareto-optimal solutions. A Pareto-optimal set is a series of solutions that are non-dominated with respect to each other. While moving from one Pareto

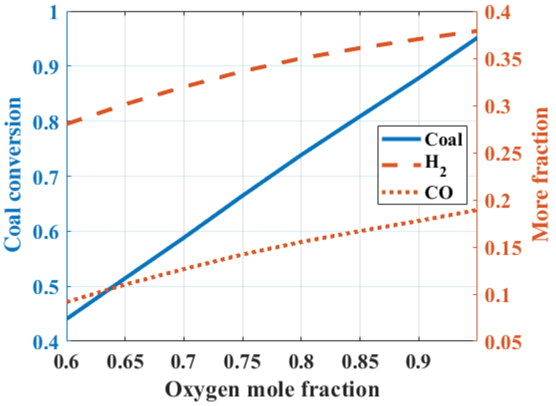

Fig. 7 – *Effects of oxygen mole fraction in inlet-air on outlet solid conversion and synthesis gas composition*

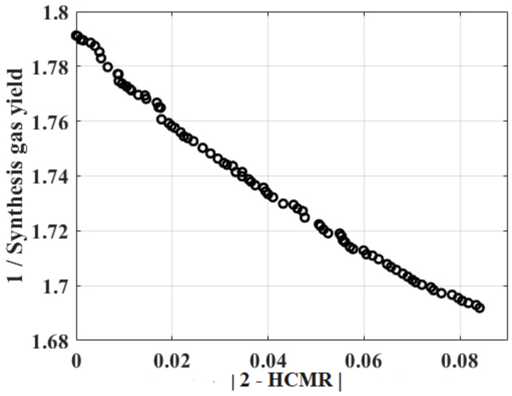

Fig. 8 – *Pareto-optimal solution set after 20,000 generations*

solution to another, there is always a certain amount of sacrifice in one objective(s) to achieve a certain amount of gain in other(s)[26].

The objective of optimization was to produce syngas with HCMR ratio of near 2 for application in methanol production with maximum yield. Therefore, the objectives included:

Objective 1:

$$\text{Minimizing}\left|2-\text{HCMR}\right| \text{ or } \left(\text{HCMR}\rightarrow 2\right) \quad (16)$$

Objective 2:

$$\begin{aligned}&\text{Minimizing}\left(1\big/\text{syngas yield}\right)\\&\text{or Maximizing}\left(\text{syngas yield}\right)\end{aligned} \quad (17)$$

where:

$$\begin{aligned}\text{syngas yield} = &\left(1-\text{carbon conversion}\right)\cdot\\&\cdot\left(\text{syngas composition}\right)\end{aligned} \quad (18)$$

subject to:

$$8 \le \text{SOR} \le 12 \quad (19)$$

$$2 \le \text{COR} \le 3 \quad (20)$$

$$550 \le \text{Inlet gas temperature}\left(\text{K}\right) \le 650 \quad (21)$$

$$18 \le \text{Reactor pressure}\left(\text{atm}\right) \le 25 \quad (22)$$

$$0.6 \le \text{Oxygen mole fraction in inlet air} \le 1.0 \quad (23)$$

Other parameters were the same as the base case. The Pareto-optimal solution sets after 20,000 generations is shown in Fig. 8. Fig. 8 shows that each solution is better than the other in one of the objective functions. Thus, the user has to decide between these solutions based on ease of operation, experience, the cost involved, and the quality of the product[26]. As it was expressed in previous sections, the HCMR ratio equal to 2 is suitable for methanol conversion unit, so the solution number 1 from Pareto-optimal solution set was chosen as the optimum solution. The optimum HCMR ratio and the syngas yield are 2.00 and 0.56, respectively. At the optimum condition, the SOR and COR ratio, inlet gas temperature, reactor pressure, and oxygen mole fraction in inlet air are 8.8, 2.3, 626 K, 23.6 atm, and 0.88 respectively. As may be observed in Table 5 (plant data), the ratio is greater than 2, and therefore not optimal for methanol production. Table 5 shows the comparison between plant data and optimum results of the present study for Pittsburgh No. 8 coal. As can be seen, the HCMR ratio is 2 and the molar flow rate of dry product gas increased 15 % in the oprimum condition relative to plant data.

Conclusions

In this study, the coal gasification process was simulated in a moving-bed reactor to achieve a temperature distribution and concentration distribution throughout the reactor in a steady state. For this purpose, the equations obtained from the mass balance and energy balance were solved, and the results compared with actual plant data that were matched with them. This simulation was useful for predicting performance of dry ash gasifier with Pittsburgh No. 8 coal as feed, and used to study the effect of SOR, COR, inlet gas temperature, rector pressure, and oxygen mole fraction in inlet air as main factors controlling the conversion and syngas composition for production of methanol. The results show that, if the reactor is to work at a higher capacity, the inlet gas temperature, reactor pressure, and oxygen mole fraction in inlet-air should be increased or COR and SOR reduced to maintain the carbon conversion and syngas yield. Increasing temperature and pressure or oxygen mole fraction in feed is associated with costs; therefore, the rational way is to reduce SOR. Finally, the reactor performance was optimized to produce the highest syngas production with a HCMR of 2, and maximum syngas yield using NSGA-II method. The optimum HCMR ratio and the syngas yield are 2.00 and 0.56, respectively.

Table 5 – *Comparison between plant data and optimum results of the present study for Pittsburgh No. 8 coal*

Parameter	Plant data	Singh *et al.*	Wen *et al.*	This work (optimum solution)
Flow rate of dry product gas (mol s^{-1})	97.10	92.36	100.29	111.7
Carbon conversion	0.989	0.980	0.983	1.00
HCMR	2.33	1.89	2.5	2.00
H_2 (% mol basis on dry gas)	39.20	37.70	40.20	38.34
CO (% mol basis on dry gas)	16.80	19.92	16.00	19.17
CO_2 (% mol basis on dry gas)	31.30	29.09	31.00	28.85
CH_4 (% mol basis on dry gas)	10.30	10.60	10.30	10.67
N_2 (% mol basis on dry gas)	1.60	1.30	1.70	2.95
H_2S (% mol basis on dry gas)	0.70	1.39	0.80	0.61

Nomenclature

a_{ij} – Stoichiometric coefficient of gas reactant *j* in reaction of *i*
A_p – Surface area of a particle
B – Correction factor for ash activity relative to the iron-based catalyst
b_{ij} – Stoichiometric coefficient of products in gas phase
C_{Pg} – Specific heat capacity of gas in constant pressure, kJ kg^{-1} K^{-1}
C_{Ps} – Specific heat capacity of solid in constant pressure, kJ kg^{-1} K^{-1}
[C] – Carbon concentration inside reactor, mol m^3
d_p – Solid particle diameter, m
E – Emissivity of coal
F – Molar flux, mol m^{-2} s^{-1}
H – Enthalpy, kJ mol^{-1}
h_p – Gas-solid heat transfer coefficient, kJ m^{-2} s^{-1} K^{-1}
R_i – Rate of i-reaction, mol m^3 s^{-1}
k_{ash} – Penetration coefficient in ash layer, mol m^3 s^{-1}
k_{film} – Penetration coefficient in gas film, mol m^3 s^{-1}
k_i – Rate constant of i^{th}-reaction, atm^{-1} s^{-1}
K_{WGS} – Equilibrium constant of water-gas shift reaction
n_p – Number of solid particles in unit of volume, m^{-3}
P – Bed pressure, atm
P_j – Partial pressure of j^{th}-component, atm
P^*_j – Equilibrium pressure of j^{th} – component, atm
R – Gas constant, atm m^3 mol^{-1} K^{-1}
S – Area of reactor wall, m^2
T – Temperature, K
X_j – Mole fraction of j^{th}-component in gas
X_{ash} – Mole fraction of ash in solid
Y – Radius of unreacted core to particle initial radius ratio
Z – Height of reactor, m
ρ_C – Density of coal, kg m^{-3}
ε_{ash} – Void fraction of solid particles
ε_{bed} – Void fraction of bed
δ – Stefan-Boltzmann constant, kJ m^{-2} K^{-4} s^{-1}

References

1. *Kulkarni, M., Ganguli, R.,* Moving bed gasification of low rank Alaska coal, J. Combust. 2012, Article ID: 918754. doi: https://doi.org/10.1155/2012/918754
2. *Bellouard, Q., Rodat, S., Abanades, S., Ravel, S., Frayssines, P.-É.,* Design, simulation and experimental study of a directly-irradiated solar chemical reactor for hydrogen and syngas production from continuous solar-driven wood biomass gasification, Int. J. Hydrogen Energ. **44** (2019) 19193. doi: https://doi.org/10.1016/j.ijhydene.2018.04.147
3. *Inaba, Y., Fumizawa, M., Tonogouchi, M., Takenaka, Y.,* Coal gasification system using nuclear heat for ammonia production, Appl. Energ. **67** (2000) 395. doi: https://doi.org/10.1016/S0306-2619(00)00037-4
4. *Bassani, A., Bozzano, G., Pirola, C., Frau, C., Pettinau, A., Maggio, E., Ranzi, E., Maneti, F.,* Sulfur rich coal gasification and low impact methanol production, J. Sustain. Dev. Energ., Water Environ. Sys. **6** (2018) 210. doi: https://doi.org/10.13044/j.sdewes.d5.0188
5. *Fernando, R.,* Developments in modelling and simulation of coal gasification, CCC/232 ISBN 2014: 978-92.
6. *Klebingat, S., Kempka, T., Schulten, M., Azzam, R., Fernandez-Steeger, T. M.,* Optimization of synthesis gas heating values and tar by-product yield in underground coal gasification, Fuel **229** (2018) 248. doi: https://doi.org/10.1016/j.fuel.2018.02.039
7. *Shadle, L. J., Berry, D. A., Syamlal, M.,* Coal conversion processes, gasification. Kirk-Othmer Encyclopedia of Chemical Technology, 2000.
8. *Azarhoosh, M. J., Halladj, R., Askari, S.,* Presenting a new kinetic model for methanol to light olefins reactions over a hierarchical SAPO-34 catalyst using the Langmuir–Hinshelwood–Hougen–Watson mechanism, J. Phys-Condens. Mat. **29** (2017) 425202. doi: https://doi.org/1361-648X/17/425202+11$33.00
9. *Azarhoosh, M. J., Halladj, R., Askari, S.,* Sonochemical synthesis of SAPO-34 catalyst with hierarchical structure

using CNTs as mesopore template, Res. Chem. Intermediat. **43** (2017) 3265.
doi: https://doi.org/10.1007/s11164-016-2824-0

10. *Azarhoosh, M. J., Halladj, R., Askari, S.*, A dynamic kinetic model for methanol to light olefins reactions over a nanohierarchical SAPO-34 catalyst: Catalyst synthesis, model presentation, and validation at the bench scale, Int. J. Chem. Kinet. **50** (2018) 149.
doi: https://doi.org/10.1002/kin.21146
11. *Yonamine, W., Thangavel, S., Ohashi, H., Fushimi, C.,* Performance analysis of a water–gas shift membrane reactor for integrated coal gasification combined cycle plant, Energ. Convers. Manage. **174** (2018) 552.
doi: https://doi.org/10.1016/j.enconman.2018.08.022
12. *Adanez, J., Labiano, F. G.,* Modeling of moving-bed coal gasifiers, Ind. Eng. Chem. Res. **29** (1990) 2079.
doi: https://doi.org/10.1021/ie00106a016
13. *Breault, R. W.*, Gasification processes old and new: A basic review of the major technologies, Energies **3** (2010) 216.
doi: https://doi.org/10.3390/en3020216
14. *Wen, C., Chen, H., Onozaki, M.,* User's manual for computer simulation and design of the moving-bed coal gasifier. Final report. West Virginia Univ., Morgantown (USA). Dept. of Chemical Engineering, 1982.
15. *Yoon, H., Wei, J., Denn, M. M.*, A model for moving-bed coal gasification reactors, AIChE J. **24** (1978) 885.
doi: https://doi.org/10.1002/aic.690240515
16. *Singh, N., Raghavan, V., Sundararajan, T.*, Mathematical modeling of gasification of high-ash Indian coals in moving bed gasification system, Int. J. Energ. Res. **38** (2014) 737.
doi: https://doi.org/10.1002/er.3078
17. *Akhlas, J., Baesso, S., Bertucco, A., Ruggeri, F.,* Coal gasification by indirect heating in a single moving bed reactor: Process development & simulation, AIMS Energ. **3** (2015) 635.
doi: https://doi.org/10.3934/energy.2015.4.635
18. *Singh, C. P. P., Saraf, D. K.,* Simulation of high-temperature water-gas shift reactors, Ind. Eng. Chem. Proc. DD. **16** (1977) 313.
doi: https://doi.org/10.1021/i260063a012
19. *Smith, B. R. J., Loganathan, M., Shantha, M. S.,* A review of the water gas shift reaction kinetics, Int. J. Chem. React. Eng. **8** (2010) 1.
doi: https://doi.org/10.2202/1542-6580.2238
20. *Belghit, A., El Issami, S.,* Hydrogen production by steam gasification of coal in gas–solid moving bed using nuclear heat, Energ. Convers. Manage. **42** (2001) 81.
doi: https://doi.org/10.1016/S0196-8904(00)00022-4
21. *Nouri, S. M. M., Ale Ebrahim, H., Jamshidi, E.,* Simulation of direct reduction reactor by the grain model, Chem. Eng. J. **166** (2011) 704.
doi: https://doi.org/10.1016/j.cej.2010.11.025
22. *Azarhoosh, M. J., Ale Ebrahim, H., Pourtarah, S. H.,* Simulating and optimizing auto-thermal reforming of methane to synthesis gas using a non-dominated sorting genetic algorithm II method, Chem. Eng. Commun. **203** (2016) 53.
doi: https://doi.org/10.1080/00986445.2014.942732
23. *Azarhoosh, M. J., Halladj, R., Askari, S.,* Application of evolutionary algorithms for modelling and optimisation of ultrasound-related parameters on synthesised SAPO-34 catalysts: Crystallinity and particle size, Prog. React. Kinet. Mech. **43** (2018) 236.
doi: https://doi.org/10.3184/146867818X15233705894446 Paper: 1700629
24. *Azarhoosh, M. J., Ale Ebrahim, H., Pourtarah, S. H.,* Simulating and optimizing hydrogen production by low-pressure autothermal reforming of natural gas using non-dominated sorting Genetic Algorithm-II, Chem. Biochem. Eng. Quart. **29** (2016) 519.
doi: https://doi.org/10.15255/CABEQ.2014.2158
25. *Lee, S., Speight, J. G., Loyalka, S. K.,* Handbook of alternative fuel technologies. CRC Press; 2014.
26. *Askari, S., Halladj, R., Azarhoosh, M. J.,* Modeling and optimization of catalytic performance of SAPO-34 nanocatalysts synthesized sonochemically using a new hybrid of non-dominated sorting genetic algorithm-II based artificial neural networks (NSGA-II-ANNs), RSC Advances **5** (2015) 52788.
doi: https://doi.org/10.1039/c5ra03764f